



## Assessment the optimal tunnel boring machine (TBM) excavation method by analyzing the stability of tunnels in squeezing rock conditions (case study: Chamshir Tunnel)

Navid Sabet<sup>1</sup>, Moreteza gharouni Nik<sup>1</sup>, Milad Alizadeh Galdiani<sup>1\*</sup>, Seyyed Ali Mosayebi<sup>1</sup>

<sup>1</sup> Department of Railway Track & Structures Engineering, School of Railway Engineering, Iran University of Science and Technology, Tehran, Islamic Republic of Iran

### ARTICLE INFO

**Article history:** (TNR 9 Bold)

Received: 21.2.2024

Accepted: 06.04.2024

Published: 05.05.2024

### Keywords:

squeezing ground  
tunneling;  
mechanized drilling  
Soil Mechanics  
TBM

### ABSTRACT

The implementation of infrastructure projects, such as tunnels, in the transportation industry is always considered one of the most expensive projects for the development of countries. One of the important issues in tunneling is the behavior that the earth exhibits in the squeezing condition. In the squeezing ground, the stones move into the tunnel and cause problems in the support and continuation of the tunnel construction. For tunneling in squeezing rock, firstly, it is necessary to know the type of phenomenon and its intensity carefully, and then design the required excavation method and support system according to the available information. In this article, it has been tried to identify the squeezing ground around tunnel and its behavior by numerical analysis. As an example, Chamshir Tunnel has been modeled for this purpose. According to the conditions of the tunnel boring machine in squeezing rock, some issues like instability of the tunnel walls, the relative flexibility of the machine in changing the excavation diameter, the supply of propulsion forces and the machine extension control, the most suitable mechanized excavation equipment should be selected and its driving force should be determined in such a way as to prevent the TBM from getting stuck inside the tunnel.

## 1. Introduction

The term "squeezing rock" has been utilized since the early days of tunnel construction in the Alps, with various definitions proposed. In essence, squeezing can be described as the displacement and convergence resulting from the accumulation and interaction of induced stresses during tunnel excavation. This phenomenon occurs when the induced shear stresses caused by excavation exceed the shear resistance of the rock mass surrounding the hole. Consequently, it can lead to increased costs, delays in project execution, and potential

damage to the concrete cover during tunnel operation. In 1946, Terzaghi presented a classification system for different rock conditions, which is utilized in estimating the loads on the retaining systems in tunnels. Terzaghi described different types of ground based on his experiences in the design and installation of steel retaining systems for railway tunnels in the Alps. Using this classification, he determined the limits of loads caused by rock pressure on retaining walls under various ground conditions. Terzaghi defines the state of squeezing rock as follows: the rock slowly advances into the tunnel without a significant increase in volume. [1] A necessary condition

\*Milad Alizadeh Galdiani  
Milad\_alizadeh@alumni.iust.ac.ir

## **Assessment the optimal tunnel boring machine (TBM) excavation method by analyzing the stability of tunnels in squeezing rock conditions (case study: Chamshir Tunnel)**

for compressibility is the presence of a high percentage of microscopic mica minerals and clay minerals with low swelling capacity.[2] The squeezing phenomenon is associated with substantial deformations and time-dependent convergence during tunnel excavation. These deformations can persist throughout excavation or extend over an extended period. Given the heightened strain in squeezing rocks compared to normal conditions, it is crucial to monitor the load on the support system to prevent any issues during its operational lifespan.[3] Additionally, TBM jamming is a significant concern during excavation in squeezing rocks, warranting investigation prior to excavation to avert damage and project delays. This preemptive measure allows for potential additional excavation by the machine if necessary. The primary objective of this article is to assess the squeezing potential of the Chamshir water transmission tunnel. It aims to estimate the load on the tunnel segments and provide an initial design for segments in squeezing zones. This evaluation will determine whether stronger segments are required in these areas or not.

### **2. Technical literature review**

In this section, the phenomenon of squeezing is defined, its historical context is explored, and various methods to investigate its severity and solutions to address it are discussed.

According to the definition provided by the International Society of Rock Mechanics (ISRM), squeezing refers to the time-dependent deformation of significant areas surrounding the tunnel, transitioning into a creep behavior if the material's shear stress threshold is surpassed. This deformation may cease upon completion of tunnel construction or persist over an extended period. Squeezing in rock during tunneling occurs when the rock is not in a stable state under pressure, leading to the displacement of rock blocks and actual stress exceeding predicted stress levels. This phenomenon is commonly observed in rocks with low axial forces and those with high fracture and displacement mechanisms. [4]

The first scientific definition for squeezing rocks was provided by Terzaghi (1946): "Squeezing rock is a rock whose entire structure has significant amounts of clay". "Squeezing rocks slowly advance into the tunnel without increasing the noticeable volume. The requirement for crumbling is the presence of a

high percentage of microscopic particles of mica or clay minerals without swelling ability". [5]

Aydan's definition of squeezing suggests that in some cases, squeezing is likened to the phenomenon of rock burst. If tunnel deformation occurs rapidly, it is categorized as a rock burst phenomenon; however, if the deformation transpires gradually, it is considered a squeezing phenomenon. [6]

The definition of squeezing provided by Gioda characterizes squeezing behavior as the gradual increase in shear deformation of a rock element over time. This phenomenon, often described as the slow advancement of plastic strains, results in limited volumetric deformation contingent upon the rock's extensibility. It is noteworthy that at times, the evolution of deformation is influenced by the creep phenomenon.[7]

The definition of squeezing provided by Singh describes it as a phenomenon wherein crushed rock mass liquefies, leading to a super-tension event. This results in the rock increasing in volume and moving into the excavated space. It is important to note that the swelling phenomenon is associated with specific materials such as montmorillonite, chlorite, etc., clays, which expand due to water absorption. However, the distinction lies in the fact that tunnel blockage due to squeezing may persist for an extended period, even up to a year, after excavation. [8] Methods for investigating squeezing potential are categorized into experimental methods, semi-experimental methods, and analytical theory methods. Based on the mechanical properties of the soil, existing stress, and strains, the extent of squeezing can be calculated. Predicting lining pressure in squeezing tunnels can be achieved through the Q and RMR methods. In the Q method, a rigid lining system can withstand smaller deformations and higher holding pressure. Conversely, a deformable support system can tolerate larger deformations and lower support pressure. Therefore, an essential parameter for estimating lining pressure is the stiffness of the lining. [9] Tunnels employing a support system of steel arches with backing, such as tunnel rubble, concrete blocks, or waste concrete, have been utilized to study the impact of support rigidity. When applying the Q system in tunneling under squeezing conditions, it becomes apparent that the stress reduction factor

(SRF) may not fully capture the effects of squeezing. However, this limitation could stem from insufficient case studies available for analysis. [10] In the second method, Goel and Jetwa proposed a relationship to estimate the retaining pressure using RMR. One of the advantages of this relationship is that it can be used for two squeezing and non-squeezing conditions, without having advanced knowledge about ground conditions. [8] Excavation methods in crumbly rocks present a significant challenge due to the substantial deformations that occur within the opening. Current investigations and research aim to facilitate tunnel excavation in squeezing rock with minimal cost and time. Traditional tunnel construction methods for openings exceeding 10 meters under squeezing conditions involve roof and face excavation, as well as the excavation of all sections, focusing on values to prevent and control large deformations during the process. [11] The use of mechanized excavation machines (TBM) in squeezing rock conditions presents several challenges. The primary issues encountered in this type of excavation include the instability of the excavation face, the limited flexibility of the machine to adjust the excavation diameter, and difficulties in providing driving forces in machines with shoes due to reduced reaction from the side steering shoes. Additionally, in soft and non-homogeneous ground conditions, controlling the machine's advancement becomes problematic. [12] One significant challenge in squeezing rock conditions is the risk of the machine getting stuck if it stops for any reason in this zone. Solutions to release the TBM from jamming include the following: Application of high-pressure mode in case of initial jamming: When the TBM stops due to necessary issues and gets jammed, excavation can be resumed by applying high-pressure mode and single mode with auxiliary jacks. This application exerts excessive pressure to help release the TBM. [13] To the device as well as segment breakage; that metal segments are used to bear the pressure from the jacks. [14] Injecting bentonite or grease on the back of the shield: In the case of low squeezing intensity, by injecting bentonite or grease on the back of the shield, they reduce the friction between the shield and the ground. The combination of two modes of high pressure and bentonite injection is also done in a more critical mode. [15] smooth blasting method: in this method, they destroy the stones behind the shield

with a gentle blast that does not cause damage to the shield and excessive vibrations. This method was used in the Swiss Gotthard tunnel to release the TBM. [16]

Manual excavation around the shield is another method employed to release the TBM from jamming. This approach involves cutting the shield and creating a gallery, ensuring proper support and safety for workers. The device is then emptied from four sides using a manual picker, and once freed, excavation can continue. This method was utilized to release the TBM in a new tunnel where jamming occurred. Similarly, in the Yellow River Diversion Tunnel, manual digging around the shield was employed to successfully release the TBM. [17]

### 3. Methodology

In This section provides an introduction to the Chamshir water transfer project, the FLAC software, and its creep behavior model. Subsequently, the process of modeling the tunnel in FLAC software for the initial design of the segment and the modeling of the TBM shield within the software is described.

The Chamshir water transfer project is a significant initiative aimed at transferring water to a designated area, involving the construction of a tunnel. To analyze the behavior of the tunnel, FLAC software is utilized. FLAC is a widely used numerical modeling software in geotechnical engineering for simulating the behavior of soil and rock under various conditions.

#### 3.1. The location and purpose of the Chamshir project

The Chamshir project is situated within the catchment area of the Zahra River, located in the southern region of the country. This catchment area extends from the Maron and Jahreh basins in the north, to the Karun and Kor rivers in the east, and to the Dilam and Gnaveh basins in the south, which are integral parts of the Hela river catchment area. The total area of the Zahra River catchment is approximately 15,349 square kilometers, comprising 11,787 square kilometers of mountainous areas and 3,652 square kilometers of foothills and plains. The average elevation of the catchment area is 950 meters above sea level.

The primary purpose of the Chamshir project is to transfer water from the Zahra River

## Assessment the optimal tunnel boring machine (TBM) excavation method by analyzing the stability of tunnels in squeezing rock conditions (case study: Chamshir Tunnel)

catchment area to meet the water demands of designated areas, thereby enhancing agricultural



Figure 1. Guide map of the studied area

activities and addressing water scarcity issues in the region. This project plays a crucial role in improving water resource management and supporting sustainable development in the surrounding areas.

The construction of Chamshir Dam and its related facilities has been done in order to store the water of the Zahra River and transfer a part of it to Dilam Plain (Lirawi). The starting point of the project is located about 70 kilometers downstream of Chamshir Dam on the Zohra River and above the confluence of the Zohra and Khairabad rivers. The free water transfer tunnel has a finished diameter of 4.6 meters and a length of 1.7 kilometers, which transfers water freely (without pressure) from the location of the dam to the end of the tunnel, and after that, the water is transferred to a diameter of 2 through a pipeline under pressure. 3.3 meters and length of 3.5 kilometers enters the hydroelectric power plant, after the power plant it is transported to the beginning of Dilam Plain by a pipe with a diameter of 2.3 meters and enters the irrigation and drainage network channels through two branches of the pipe to the location of construction units 1 and 3.

The map in figure 1 corresponds to Bushehr Province, a coastal region situated in the southern part of Iran, characterized by its proximity to the Persian Gulf. Within the depicted figure, the trajectory of the tunnel is

clearly delineated, signifying a pivotal aspect of scientific inquiry into the region's geological and infrastructural features.

### 3.2. tunnel excavation

There are numerous factors that influence the selection of a tunnel implementation method. These include the geological conditions along the tunnel route, the length and intended use of the tunnel, the cross-section design, the potential for geological hazards, accessibility to the tunnel site, availability of skilled labor, project costs, implementation schedule, as well as political and economic conditions. Each of these factors plays a significant role in determining the most suitable method for implementing the tunnel project. Finally, based on the outlined cases, mechanized excavation was carried out utilizing a horseshoe-shaped mold. In the traditional and semi-mechanized excavation methods, which involve the use of an arm machine for tunneling, the excavation section is shaped like a horseshoe with dimensions of 1.6 meters in width and height, resulting in an excavation area of approximately 32.2 square meters. Following the application of concrete covering, the tunnel achieves finished dimensions of 4.5 meters in both width and height. In the full-section excavation method or TBM (Tunnel Boring Machine), the excavation cross-section is circular with a diameter of 3.5 meters, yielding a cross-sectional area of 1.22 square meters. Therefore, the selected TBM must have the capability to excavate a tunnel with a diameter of at least 3.5 meters. Additionally, due to excavation in clay and marl layers, the chosen device should be equipped with a gauge cutter to enable additional excavation of up to 10 cm.

### 3.3. Numerical modeling

The foundation of numerical methods lies in transforming an environment with infinite degrees of freedom into a system with limited degrees of freedom at specific points within the environment. By analyzing the influence of loading forces at these points and determining their respective deformations, the deformation at other points can be obtained through interpolation techniques.[18] The location, number, and interrelationship of these points are determined by the elements within the environment. Each element represents a small portion of the environment with its unique geometric properties and material characteristics. These elements are connected to

each other to form a mesh that represents the entire system. Through this mesh, the behavior of the entire structure can be analyzed by examining the interactions and deformations of the individual elements. After dividing the medium into relatively small elements, the characteristic equations of the elements are solved simultaneously.[19] Numerical methods are divided into different methods such as finite differences, finite elements, discrete elements, boundary elements, etc., with the advancement of computers, programming has been done for each of these methods. In relation to geotechnical and mineral issues, there are many programs that use the FLAC ver.7.00.411 program in this regard. This program is based on finite difference method. The specifications and required parameters of the CVISC viscoelastic plastic creep model are listed in Table No. 1. It should be noted that among the required parameters of this model are adhesion, density, internal friction angle, expansion angle, tensile limit and elastic shear modulus. They have been obtained using on-site tests and tests.

Table 1. Model properties

| Property                   | Index in FLAC |
|----------------------------|---------------|
| Elastic Bulk modulus       | b             |
| Cohesion                   | C             |
| Mass density               | de            |
| Dilation angel             | di            |
| Angel of internal friction | f             |
| Kelvin shear Modulus       | k-s           |
| Kelvin Viscosity           | k-v           |
| Elastic shear Modulus      | sh            |
| Tension limit              | t             |
| Maxwell Viscosity          | Vis           |

Table 1 provides a comprehensive list of intrinsic properties and corresponding indices within the model. It serves as a foundational reference aiding in the identification and analysis of critical attributes essential for modeling processes and interpretations.

To achieve the desired tunnel geometry in FLAC, it is recommended to simulate the rock mass with dimensions approximately 10 times the diameter of the tunnel. This approach helps minimize the influence of boundary conditions on the analysis results, especially in cases where displacements are of particular importance. Furthermore, to expedite the analysis process and considering the program's limitations in selecting a large number of meshes, a total of 10,000 elements were chosen. This balance

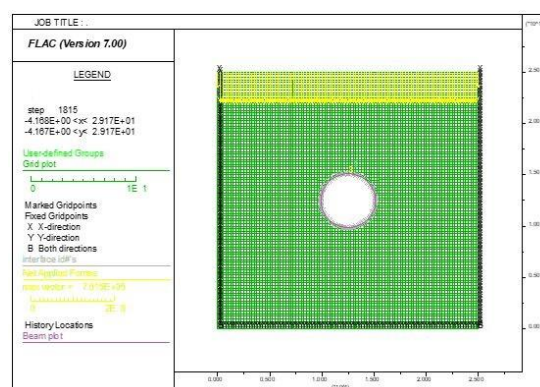


Figure 2. Tunnel model geometry in FLAC

between dimensions and element count aims to ensure an efficient and accurate analysis of the tunnel behavior within the FLAC program. In implementing the desired tunnel geometry within the FLAC 2D software, the remaining overhead was applied to the model using the "Apply" command. This involved applying a stress of approximately 150 meters of rock mass to the surface, with support conditions set as "Fix." Subsequently, the "Initial" command was utilized to apply stresses to the rock mass, increasing proportionally with depth. To create the desired tunnel geometry, a circle with a radius of 2.65 was generated at the center of the mesh using the "Circle" command in FLAC 2D. This circle represents the cross-section of the tunnel and serves as the basis for the subsequent analysis of the tunnel behavior within the software. The opening of the tunnel is executed in a space consisting of 22 elements according to figure 2. At this stage, the program was run to create deformations resulting from the application of in situ stress and the creation of the tunnel cavity before assigning the proposed model., and the final analysis is in the geometry and real conditions of the ground. Simulated. In order to simulate the real conditions of the ground and the rock mass, Berger's creep model (CIVISC) is assigned to the mentioned geometry, and then the piece with the order of Beam with a thickness of 250 mm and its injection grout with the order of interface with a thickness of 10 mm. Once again, the model was pre-partitioned and built with a machine bumper. The distance between the shield and the piece was considered to be 30 mm, and this model was implemented to determine whether the creep phenomenon in the two squeezed areas of the tunnel exerts a force on the shield of the device that causes the device to jam.

## Assessment the optimal tunnel boring machine (TBM) excavation method by analyzing the stability of tunnels in squeezing rock conditions (case study: Chamshir Tunnel)

The figure 2 intricately details the tunnel modeling conducted via FLAC software, meticulously showcasing the geometric intricacies of the tunnel itself, as well as its environmental context.

The desired software should be calibrated to determine whether the results obtained from it can be cited. Therefore, by modeling a research tunnel called Quatre Chemins and controlling the results obtained from the software by comparing with the results of analytical relations for this tunnel, the accuracy of the numerical analysis results is checked.

Pane et al. proposed a series of relations for time-dependent tunnel convergence. In order to control the correctness of their proposed relationships, they used the results of Quatre Chemins tunnel instrumentation. [20]This

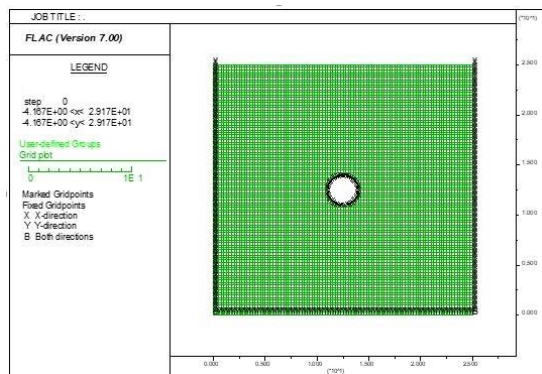


Figure 3. The tunnel model created in the FLAC with x and y axis boundary conditions, the dimensions of the model are in 10 meters.

tunnel is a circular tunnel with a radius of  $r = 1.5\text{m}$ , which was built at a depth of 85 meters from the ground in a 38-meter-long marl mass for research purposes. The characteristics of the marl mass are shown in Table No. 2

Table 2. Mechanical characteristics of Quatre Chemins tunnel rock mass

| $\sigma_c$ (MPa) | C (MPa) | $\phi$ | $\nu$ | E (MPa) |
|------------------|---------|--------|-------|---------|
| 2                | 0.5     | 30     | 0.4   | 360     |

This table presents a detailed overview of the mechanical properties inherent to the rock mass within the Quatre Chemins tunnel.

Table 3. Creep parameters input to the software for time-dependent analysis.

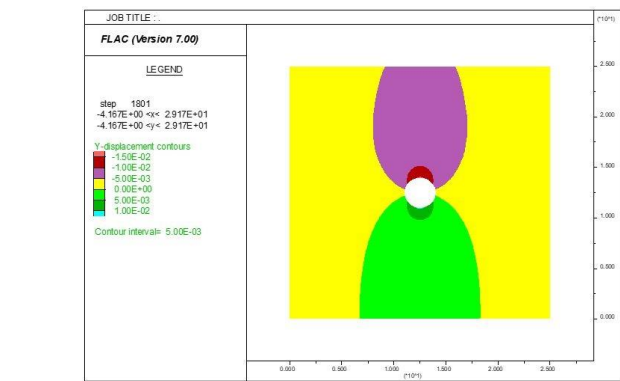


Figure 4. Displacement contours in the Y direction (on the tunnel wall, the amount of displacement is 15 mm).

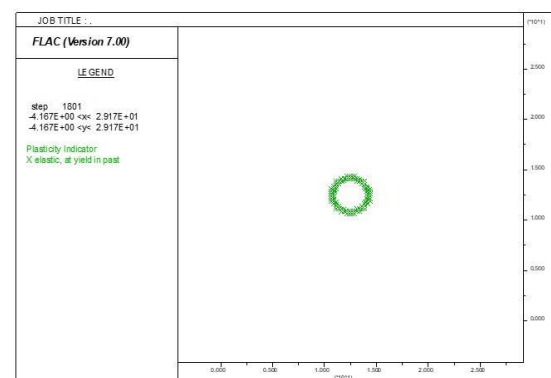


Figure 5. Showing the plasticized areas around the tunnel (radius of the plastic area is about 2.2 meters).

| $\eta_2$<br>(MP – Year) | $\eta_1$<br>(MPa – Year) | G2<br>(MPa) | G1<br>(MPa) |
|-------------------------|--------------------------|-------------|-------------|
| 36.5                    | 0.137                    | 128.57      | 50          |

Table 3 presents the parameters utilized as input for time-dependent analysis regarding creep behavior within the software framework.

Given the specifications presented in Tables 2 and 3, the software has been scrutinized for its tunnel analysis capabilities and performance, serving as inputs for the evaluation process.

For the tunnel, a creep analysis has been done with the CVISC model, taking into account the effect of time, and the related results are given in following.

For tunnel analysis considering time, the condition of radial symmetry should be considered by ignoring the weight of the loose mass in the top of the tunnel. The shape of the tunnel model in the software is according to figure number2. [21]

Fig. 3. The tunnel model created in the FLAC with x and y axis boundary conditions, the dimensions of the model are in 10 meters.

By performing the analysis on the model, the amount of displacement of the tunnel is according to figure 4.

In figures 4 and 5, the display illustrates the results of numerical analysis for radial displacements of the specified tunnel. Geological units' SST and MMT are examined with various tunneling coefficients (K). The measured radial displacements categorize the modeling results of the tunnel into "Low squeezing" and "Non-squeezing" conditions. Additionally, the visualizations indicate that the radial displacement of tunnels is contingent on the differences in geological units and various conditions. For ease of comparison, the values are also provided in Table 7.

Table 4. The results of moving Paneh's analytical method and numerical analysis

| Analytical method | Numerical method |                            |
|-------------------|------------------|----------------------------|
| 1.5               | 1.5              | Radial displacement (cm)   |
| 2.19              | 2.2              | Radius of plastic zone (m) |

According to table 4, the comparison between the analytical and numerical methods reveals close agreement in the assessment of certain critical parameters. Specifically, in the context of radial displacement, both methods demonstrate a congruence with values of 1.5 cm, highlighting a consistent estimation of this particular deformation aspect.

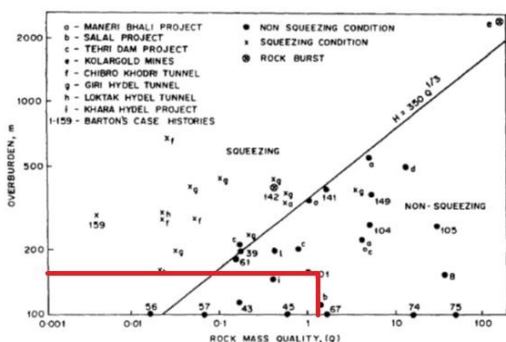


Figure 6. Investigation of squeezing by Singh's method for SST unit

The distribution of plasticized areas of the tunnel is shown in Figure 5. According to the figure, the radius of the plasticized area can be read.

#### 4. Analysis of the results

In this section, the intensity of squeezing has been investigated with experimental, semi-experimental and analytical methods; Also, by modeling the tunnel in FLAC software, the bending moment and axial force on the support system have been estimated for the initial design of the segment, and it can be seen that the proposed cover has shown good performance against static loading and will be stable under the incoming loads. At the end, by checking the forces acting on the shield of the device in FLAC software, the possibility of the device getting stuck has been checked for 1 week.

Experimental method According to geological studies, the sink method has been predicted in this squeezing phenomenon in both SST and MMT regions. Since the Q classification is for jointed rocks. Here, due to having the information of the seams related to the SST unit and considering that the experimental methods (Singh and Goel) are dependent on Q, Only the SST unit can be evaluated for squeezing using these two methods.

$$H = 350(1.78)^{1/3} = 424.171 \tag{1}$$

Critical overhead

$$H=166$$

In this section, the examination of the squeezing conditions is initially addressed using the Singh method. Considering the tunnel conditions, the overhead, and the relevant diagrams (Fig. 6), it is determined that the tunnel is in a non-squeezing state.

$$N = (Q)_{SRF=1} = 4.45 , B=5.1 \tag{2}$$

$$H = (275(4.45)^{0.33})5.1^{-0.1} = 382.41$$

Critical overhead

**Assessment the optimal tunnel boring machine (TBM) excavation method by analyzing the stability of tunnels in squeezing rock conditions (case study: Chamshir Tunnel)**

$$H=166$$

The assessment of tunnel squeezing using Goel's method is illustrated in Figure 7. Considering both the overhead conditions and the characteristics of the soil, the tunnel is classified as non-squeezing. The calculation using the Singh method is based on the critical strain equation number 3. The value is determined according to the soil type and critical strain, as calculated below. The results indicate that this method considers the tunnel as squeezing.

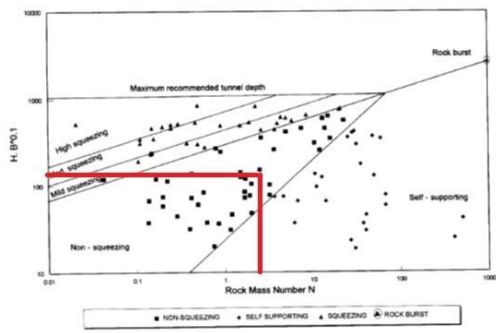


Figure 7. Checking the squeezing by Goel's method for SST unit.

$$\varepsilon_{Cr} = 5.84 \frac{(\sigma_{ci})^{0.88}}{E_i^{0.63} Q^{0.12}} = 0.53 \quad \frac{u_a}{a} = 0.55 \quad (3)$$

$$SI = \frac{\text{Observed or expected strain}}{\text{Critical strain}} = \frac{\frac{u_a}{a}}{\varepsilon_{cr}} = \frac{0.55}{0.53} = 1.05 \quad (4)$$

Applying Jetwa et al.'s method to both the SST and MMT units, a squeezing assessment has been carried out. The results derived from this method (equation 5) indicate that the tunnel exhibits a condition of "low squeezing" for SST and "medium squeezing" for MMT. This suggests that, according to Jetwa et al.'s method, the level of squeezing in the SST unit is relatively low, providing valuable insights into the tunnel's behavior under specific geological and stress conditions. The differential squeezing assessments for SST and MMT highlight the method's ability to discern variations in squeezing potential across different geological units.

For the SST unit

$$N_c = \frac{\sigma_{cm}}{p_0} = \frac{\sigma_{cm}}{\gamma H} = \frac{2.94 \cdot 10^6}{3.5192 \cdot 10^6} = 0.835 \quad (5)$$

low squeezing

For the MMT unit

$$N_c = \frac{\sigma_{cm}}{p_0} = \frac{\sigma_{cm}}{\gamma H} = \frac{1.561 \cdot 10^6}{3.319 \cdot 10^6} = 0.49$$

The analysis using Aidan's method for the SST unit has been conducted, and the results reveal a condition of "high squeezing." This assessment, based on Aidan's method, suggests that the SST unit exhibits a notable degree of squeezing behavior. This finding holds significance in understanding the tunnel's response to geological and stress factors, particularly when considering the potential challenges associated with high squeezing conditions.

$$\eta_p = \frac{\varepsilon_p}{\varepsilon_e} = 2\sigma_{ci}^{-0.17} = 1.2 \text{ Mpa}$$

$$\eta_s = \frac{\varepsilon_s}{\varepsilon_e} = 3\sigma_{ci}^{-0.25} = 1.42 \text{ Mpa}$$

$$\eta_f = \frac{\varepsilon_f}{\varepsilon_e} = 5\sigma_{ci}^{-0.32} = 1.92 \text{ Mpa}$$

$$\varepsilon_{\theta}^a = \frac{\sigma_{\theta}}{E_m} = \frac{4.7}{1.307 \cdot 10^3} = 0.00359$$

$$\varepsilon_{\theta}^e = \frac{\sigma_{cm}}{E_m} = \frac{2.94}{1.307 \cdot 10^3} = 0.00224$$

$$\frac{\varepsilon_{\theta}^a}{\varepsilon_{\theta}^e} = 1.602 \quad \text{high squeezing}$$

The evaluation using the Hooke and Marinos method for the SST unit indicates a calculated value of  $\varepsilon_t=0.0062$ . This result categorizes the SST unit as "non-squeezing," suggesting that the tunnel in this geological unit is not prone to squeezing conditions.

$$\varepsilon_t = 0.0062 < 1 \quad \text{non-squeezing}$$

For the MMT unit

$$\varepsilon_t = 0.0222 < 1 \quad \text{non-squeezing}$$



Utilizing Barla's method for the SST, this tunnel falls within the range associated with "low squeezing." This implies that, according to Barla's method, the SST unit is characterized by low squeezing conditions. Similarly, for the MMT, this tunnel also falls within the range indicative of "low squeezing." Thus, based on Barla's method, the MMT unit is also characterized by low squeezing conditions.

$$\sigma_{cm} = 2.94$$

$$P0=3.519$$

$$\frac{\sigma_{cm}}{p_0} = 0.835 \quad \text{low squeezing}$$

For the MMT unit

$$\sigma_{cm} = 1.561$$

$$P0=3.13$$

$$\frac{\sigma_{cm}}{p_0} = 0.498 \quad \text{low squeezing}$$

According to the ISRM (International Society for Rock Mechanics) method, the evaluation for the SST unit indicates a classification of "low squeezing." Similarly, for the MMT unit, the ISRM method results in a categorization of "low squeezing" as well. These outcomes suggest that, based on the criteria defined by the ISRM method, both the SST and MMT units exhibit a relatively low potential for squeezing

$$\sigma_{\theta} = 5.278$$

$$P0=3.519$$

$$\frac{\sigma_{\theta}}{p_0} = 1.499 \quad \text{low squeezing}$$

For the MMT unit

$$\sigma_{\theta} = 4.708$$

$$P0=3.13$$

$$\frac{\sigma_{\theta}}{p_0} = 1.504 \quad \text{low squeezing}$$

Various methods have been employed for the analysis of tunnel squeezing. Below, table

number 5 has been provided for the comparison of results obtained from these methods.

Table 5. Summary of the obtained results for squeezing conditions based on the investigated methods.

| Sections                                | MMT | SST |
|---|-----|-----|
| Singh's method                          | -   | NS  |
| Goel method                             | -   | NS  |
| Singh's method based on critical strain | -   | S   |
| Jetwa's method                          | MS  | S   |
| Aidan's method                          | HS  | HS  |
| Hooke and Marinos method                | NS  | NS  |
| Barla's method                          | S   | S   |
| ISRM method                             | S   | S   |
| Mean                                    | S   | S   |

This comprehensive overview in Table number 5 suggests that the MMT section generally tends towards squeezing conditions across various methods, while the SST section exhibits more variability in the assessed squeezing potential. The combination of these findings provides a nuanced understanding of the tunnel behaviour in different geological contexts. Further analysis and consideration of these results in the context of project requirements and safety considerations will be crucial for informed decision-making. The intensity of squeezing using the radial strain obtained from the numerical method Using the strain obtained from FLAC, the phenomenon of squeezing in SST and MMT unit was investigated with (K=0.4, 1, 1.5), and the results are as described in Table 7.

**Assessment the optimal tunnel boring machine (TBM) excavation method by analyzing the stability of tunnels in squeezing rock conditions (case study: Chamshir Tunnel)**

Table 6. Degree of squeezing based on tunnel radial strain.

| Classification number | level of squeezing | Radial strain of the tunnel |
|-----------------------|--------------------|-----------------------------|
| 1                     | Non-squeezing      | $\epsilon_t \leq 1$         |
| 2                     | Low squeezing      | $1 < \epsilon_t \leq 2.5$   |
| 3                     | High squeezing     | $2.5 < \epsilon_t \leq 5$   |
| 4                     | Too much squeezing | $5 < \epsilon_t \leq 10$    |
| 5                     | Severe squeezing   | HS                          |

The table 6 illustrates the classification of soil types based on their deformability by measuring radial strains in tunnels. The level of deformability is divided into five categories ranging from low deformability to very severe deformability. In other words, table 6 delineates a comprehensive classification of tunnel squeezing based on radial strain, offering a nuanced perspective on the severity of deformation. In the context of this table, "Non-squeezing" (Level 1) characterizes tunnels with a radial strain ( $\epsilon_t$ ) of 1 or less, indicating minimal deformation. Moving to "Low Squeezing" (Level 2), radial strains between 1

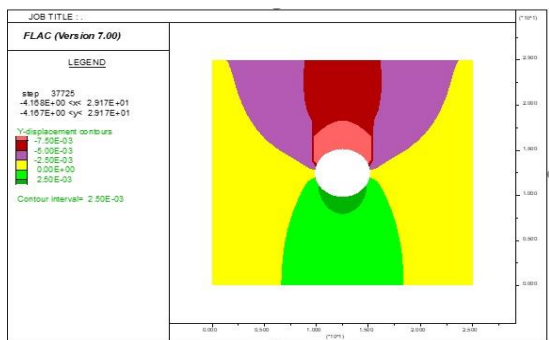


Figure 7. Time-independent tunnel displacement contour Y directions (SST unit, K=0.4, step=3773)

and 2.5 are indicative of moderate deformation. "High Squeezing" (Level 3) denotes more significant strain, falling within the range of 2.5 to 5. For more severe cases, "Too Much Squeezing" (Level 4) involves strains from 5 to 10, suggesting substantial deformation. Finally, "Severe Squeezing" (Level 5) is denoted as HS, signifying strains surpassing 10.

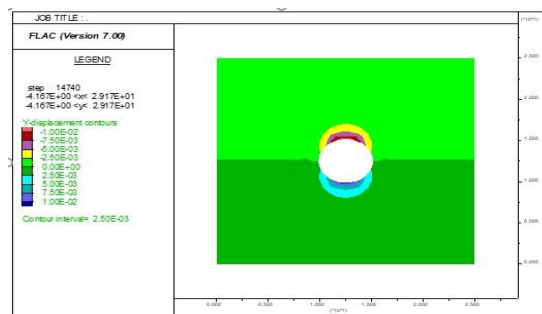


Figure 8. Time-independent tunnel displacement contour Y directions (SST unit, K=0.4, step=3773)

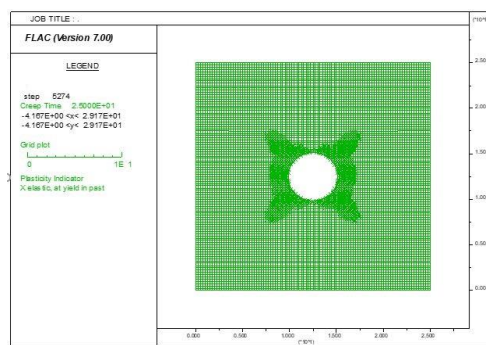


Figure 9. Expanding the plastic zone around the tunnel (SST unit and K=0.4).

Table 7. Radial strain obtained from numerical analysis.

| Geology unit | K   | Radial strain | level of squeezing |
|--------------|-----|---------------|--------------------|
| SST          | 0.4 | 0.36          | NS                 |
| SST          | 1   | 0.35          | NS                 |
| SST          | 1.5 | 0.55          | NS                 |
| MMT          | 0.4 | 1.12          | NS                 |
| MMT          | 1   | 0.98          | NS                 |
| MMT          | 1.5 | 1.61          | NS                 |

The table 7 outlines data on geological units

(SST and MMT), their associated coefficients (K), radial strain percentages, and squeezing levels denoted as "NS." The radial strain percentage signifies the change in rock diameter under increasing radial pressure. The "NS" squeezing level requires additional context for precise interpretation. This table offers insights into the deformation behavior of rocks across different geological units and pressure conditions.

The conducted analysis on the model indicates that the number of displacements in both the Y directions remains independent of time, as evidenced by the observations gleaned from Figure 8 and 9. These figures portray a consistent trend wherein the displacements exhibit no discernible variation over time.

Rock load and how to calculate it by numerical method, the load by the plastic zone is considered as the Rock load on the support system by calculating the plastic area by the software according to figure 10. And the output of the software is summarized in Table No. 8.

The plastic deformation zone surrounding the tunnel is confined within a specific radius. The modeling approach has been expanded to encompass a space exceeding threefold, aiming to enhance the reliability of the obtained outcomes. The plastic zone configuration signifies that the most substantial effects manifest in the regions situated above the right and left sides of the tunnel.

Table 8. Estimation of maximum Rock load for different units along the tunnel based on numerical method.

| Description        | Rock Load (ton/m <sup>2</sup> ) | Stress condition (K) | Geology unit |
|--------------------|---------------------------------|----------------------|--------------|
| Maximum overburden | 3.18                            | 0.4                  | SST          |
|                    | 3.71                            | 1                    |              |
|                    | 5.3                             | 1.5                  |              |
| Maximum overburden | 6.98                            | 0.4                  | MMT          |
|                    | 7.52                            | 1                    |              |
|                    | 11.28                           | 1.5                  |              |

Table 8 illustrates the estimation of maximum rock load (in tons per square meter) for different units along the tunnel employing a numerical method. The estimations are based on stress conditions (K values) and associated geology units across various section numbers.

For the SST (Support-Squeeze Test) unit at Section 1, the estimated rock load values range between 3.18 and 5.3 tons per square meter based on different stress conditions. Similarly, for the MMT (Massive Mudstone Test) unit at Section 1, the estimated rock load values vary from 6.98 to 11.28 tons per square meter concerning different stress conditions.

These estimations serve as pivotal metrics for evaluating the load-bearing capacity and stress distribution within the tunnel's geological units, aiding in structural assessments and design considerations.

## 5. Conclusion

The excavation of tunnels using mechanized methods is among the costliest aspects of infrastructure projects. Planning for the operation of Tunnel Boring Machines (TBMs) and implementing measures to prevent the machine from becoming stuck in squeezing ground conditions are of utmost importance. In this article, the squeezing potential of the Chamshir tunnel was investigated using a combination of experimental, semi-experimental, and analytical methods.

Furthermore, the tunnel was modeled in FLAC software and data analysis was conducted to calculate the rock load on the segment, taking into account the expansion of the plastic zone. This comprehensive approach allowed for a thorough assessment of the tunnel's behavior in squeezing rock conditions and facilitated the calculation of the load on the tunnel segment. The findings from this study contribute valuable insights into the efficient and safe operation of TBMs in challenging geological conditions.

The results obtained from this article, utilizing empirical, semi-empirical, and analytical formulas, indicate that in the two geological units prone to squeezing, namely SST and MMT, with the assumed horizontal to vertical stress ratio, the probability of squeezing is evaluated as low to moderate. This assessment provides valuable insights into the potential challenges and risks associated with tunneling in these geological conditions. By evaluating the

## Assessment the optimal tunnel boring machine (TBM) excavation method by analyzing the stability of tunnels in squeezing rock conditions (case study: Chamshir Tunnel)

squeezing potential through various methods, this study offers a comprehensive understanding of the feasibility and safety considerations for tunnel excavation in the Chamshir tunnel project.

The The diverse results obtained from the experimental, semi-experimental, and analytical methods highlight the variation between these approaches in determining the squeezing potential. Among these methods, Aidan's method appears to be more conservative in its estimates.

Considering the suitability of the proposed segment for areas prone to squeezing, it can be concluded that there is no necessity to utilize high-load segments in these regions. The segment designed for non-squeezing units can adequately function in squeezing areas as well.

In the geological unit of MMT, if the stress ratio (K) is equal to 1.5, there is a possibility of the TBM machine getting stuck. To ensure operational safety, an additional 20 millimeters of excavation should be carried out in this geological unit. This precautionary measure will help mitigate the risk of the TBM encountering difficulties or becoming stuck during excavation in the MMT geological unit.

## 6. References

[1] H. Ma, G. Han, L. Peng, L. Zhu, and J. Shu, "Rock thin sections identification based on improved squeeze-and-Excitation Networks model," *Comput. Geosci.*, vol. 152, p. 104780, 2021, doi: <https://doi.org/10.1016/j.cageo.2021.104780>.

[2] A. Jain and K. S. Rao, "Empirical correlations for prediction of tunnel deformation in squeezing ground condition," *Tunn. Undergr. Sp. Technol.*, vol. 125, p. 104501, 2022, doi: <https://doi.org/10.1016/j.tust.2022.104501>.

[3] W. Liu et al., "Long-term stress monitoring and in-service durability evaluation of a large-span tunnel in squeezing rock," *Tunn. Undergr. Sp. Technol.*, vol. 127, p. 104611, 2022, doi: <https://doi.org/10.1016/j.tust.2022.104611>.

[4] A. Ketan, G. Marte, and H. Ahmadreza, "Physical Modeling of Lined Tunnel in Squeezing Ground Conditions," *Geo-Congress 2020*. pp. 335–344, Feb. 21, 2020, doi: [doi:10.1061/9780784482797.033](https://doi.org/10.1061/9780784482797.033).

[5] K. Guan, W. Zhu, X. Liu, J. Wei, and L. Niu, "Re-profiling of a squeezing tunnel considering the post-peak behavior of rock mass," *Int. J. Rock Mech. Min. Sci.*, vol. 125, p. 104153, 2020, doi: <https://doi.org/10.1016/j.ijrmms.2019.104153>.

[6] C. Zhang, G. Cui, Y. Zhang, H. Zhou, N. Liu, and S. Huang, "Squeezing deformation control during bench excavation for the Jinping deep soft-rock tunnel," *Eng. Fail. Anal.*, vol. 116, p. 104761, 2020, doi: <https://doi.org/10.1016/j.engfailanal.2020.104761>.

[7] "Finite element analysis of tunnel behaviour in squeezing ground: Liang, R Y K; Sobhanie, M Proc Ninth Danube-European Conference on Soil Mechanics and Foundation Engineering, Budapest, 2–5 October 1990P337–343. Publ Budapest: Akademiai Kiado, 1990," *Int. J. Rock Mech. Min. Sci. Geomech. Abstr.*, vol. 29, no. 5, p. 327, 1992, doi: [https://doi.org/10.1016/0148-9062\(92\)93055-O](https://doi.org/10.1016/0148-9062(92)93055-O).

[8] M. Zhao, J. M. de Oliveira Barbosa, A. V Metrikine, and K. N. van Dalen, "Semi-analytical solution for the 3D response of a tunnel embedded in an elastic half-space subject to seismic waves," *Soil Dyn. Earthq. Eng.*, vol. 174, p. 108171, 2023, doi: <https://doi.org/10.1016/j.soildyn.2023.108171>.

[9] P. Pantaweesak, P. Sontamino, and D. Tonnayopas, "Alternative software for evaluating preliminary rock stability of tunnel using rock mass rating (RMR) and rock mass quality (Q) on android smartphone," *Eng. J.*, vol. 23, no. 1, pp. 95–108, 2019, doi: [10.4186/ej.2019.23.1.95](https://doi.org/10.4186/ej.2019.23.1.95).

[10] P. Puichaisorn and B. Sangpetngam, "Permanent Deformation Behavior under Repeated Load of Recycled Material Stabilized with Bitumen Emulsion," *Eng. J.*, vol. 26, no. 4, pp. 13–23, 2022, doi: [10.4186/ej.2022.26.4.13](https://doi.org/10.4186/ej.2022.26.4.13).

[11] K. Arora, M. Gutierrez, and A. Hedayat, "Physical model simulation of rock-support interaction for the tunnel in squeezing ground," *J. Rock Mech. Geotech. Eng.*, vol. 14, no. 1, pp. 82–92, 2022, doi: <https://doi.org/10.1016/j.jrmge.2021.08.016>.

[12] M. Esmail, H. Khajehei, and F. Astaraki, "The Effectiveness of Deep Soil Mixing on Enhanced Bearing Capacity and Reduction of Settlement on Loose Sandy Soils

- TT -,” IJRARE, vol. 4, no. 2, pp. 33–39, Oct. 2017, doi: 10.22068/IJRARE.4.2.33.
- [13] M. Esmaeili, V. Khalilian, and F. Khatibi, “A Numerical Study on Geof foam Application in the Settlement Reduction of Railway Embankments TT -,” IJRARE, vol. 4, no. 1, pp. 13–27, Mar. 2017, doi: 10.22068/IJRARE.4.1.13.
- [14] F. Mezger, M. Ramoni, G. Anagnostou, A. Dimitrakopoulos, and N. Meystre, “Evaluation of higher capacity segmental lining systems when tunnelling in squeezing rock,” *Tunn. Undergr. Sp. Technol.*, vol. 65, pp. 200–214, 2017, doi: <https://doi.org/10.1016/j.tust.2017.02.012>.
- [15] Q. Yan, C. Zhang, W. Wu, H. Zhu, and W. Yang, “3D Numerical Simulation of Shield Tunnel Subjected to Swelling Effect Considering the Nonlinearity of Joint Bending Stiffness,” *Period. Polytech. Civ. Eng.*, vol. 63, no. 3 SE-Research Article, pp. 751–762, Sep. 2019, doi: 10.3311/PPci.13996.
- [16] J.-Z. Zhang and X.-P. Zhou, “Time-dependent jamming mechanism for Single-Shield TBM tunneling in squeezing rock,” *Tunn. Undergr. Sp. Technol.*, vol. 69, pp. 209–222, 2017, doi: <https://doi.org/10.1016/j.tust.2017.06.020>.
- [17] S. Goodarzi, J. Hassanpour, S. Yagiz, and J. Rostami, “Predicting TBM performance in soft sedimentary rocks, case study of Zagros mountains water tunnel projects,” *Tunn. Undergr. Sp. Technol.*, vol. 109, p. 103705, 2021, doi: <https://doi.org/10.1016/j.tust.2020.103705>.
- [18] W. Lu et al., “Study on mechanical properties of composite support structures in TBM tunnel under squeezing soft rock conditions,” *Tunn. Undergr. Sp. Technol.*, vol. 144, p. 105530, 2024, doi: <https://doi.org/10.1016/j.tust.2023.105530>.
- [19] G. Ma, Z. He, C. He, X. Kang, S. Wang, and G. Xu, “Time-dependent performance assessment of mountain tunnels considering the hazards associated with squeezing soft rock and nonuniform steel corrosion in RC lining structure,” *Comput. Geotech.*, vol. 164, p. 105808, 2023, doi: <https://doi.org/10.1016/j.compgeo.2023.105808>.
- [20] T. Wan, P. Li, H. Zheng, and M. Zhang, “An analytical model of loosening earth pressure in front of tunnel face for deep-buried shield tunnels in sand,” *Comput. Geotech.*, vol. 115, p. 103170, 2019, doi: <https://doi.org/10.1016/j.compgeo.2019.103170>.
- [21] X. Xu, Z. Wu, and Q. Liu, “An improved numerical manifold method for investigating the mechanism of tunnel supports to prevent large squeezing deformation hazards in deep tunnels,” *Comput. Geotech.*, vol. 151, p. 104941, 2022, doi: <https://doi.org/10.1016/j.compgeo.2022.104941>.